Control and measurement of three-qubit entangled states

C. F. Roos[1], M. Riebe[1], H. Häffner[1], W. Hänsel[1], J. Benhelm[1], G. P.T. Lancaster[1], C. Becher[1], F. Schmidt-Kaler[1] & R. Blatt[1,2]

[1]*Institut für Experimentalphysik, Universität Innsbruck, Technikerstraße 25, A-6020 Innsbruck, Austria*

[2]*Insitut für Quantenoptik und Quanteninformation, Österreichische Akademie der Wissenschaften, Technikerstraße 25, A-6020 Innsbruck, Austria*

We report the deterministic creation of maximally entangled three-qubit states, specifically the Greenberger-Horne-Zeilinger (GHZ) state and the W-state, with a trapped ion quantum computer. We demonstrate the selective readout of one qubit of the quantum computer and show how GHZ- and W-states are affected by this local measurement. Additionally, we demonstrate conditional operations controlled by the results from selectively reading out one qubit. Tripartite entanglement is deterministically transformed into bipartite entanglement by local operations only. These operations are the measurement of one qubit of a GHZ-state in a rotated basis and -conditioned upon the result- the application of single qubit rotations.

Quantum information processing rests on the ability to deliberately initialize, control, and manipulate a set of quantum bits forming a quantum register (1). Carrying out an algorithm then consists of sequences of quantum gate operations which generate multi-partite entangled states of this quantum register. Eventually, the outcome of the computation is obtained by measuring the state of the individual quantum bits. For the realization of some important algorithms, such as quantum error correction (1,2,3,4,5), and for teleportation (6), a subset of the quantum register must be selectively read out and subsequent operations on other qubits have to be conditioned on the measurement result.

The capability of entangling a scalable quantum register is the key ingredient for quantum information processing as well as for many-party quantum communication. While entanglement with two or more qubits has been demonstrated in a few experiments (7,8,9,10,11,12) the experiments described below allow the deterministic generation of 3-qubit entangled states and the selective read-out of an individual qubit followed by local quantum operations conditioned on the read-out.

The experiments are performed in an elementary ion-trap quantum processor (13,14). For the investigation of tripartite entanglement (15,16,17) we trap three $^{40}Ca^{+}$ ions in a linear Paul trap. Qubits are encoded in a superposition of the $S_{1/2}$ ground state and the metastable $D_{5/2}$ state (lifetime $\tau \approx 1.16$s). Each ion-qubit is individually manipulated by a series of laser pulses on the $S \equiv S_{1/2}$ (m_j=-1/2) to $D \equiv D_{5/2}$ (m_j=-1/2) quadrupole transition near 729 nm employing narrowband laser radiation tightly focussed onto individual ions in the string. The entire quantum register is prepared by Doppler cooling, followed by sideband ground state cooling of the center-of-mass vibrational mode ($\omega = 2\pi \times 1.2$ MHz). The ions' electronic qubit states are initialised in the S-state by optical pumping.

Three qubits can only be entangled in two inequivalent ways, for which the Greenberger-Horne-Zeilinger (GHZ) state, $|GHZ\rangle = 1/\sqrt{2}\,(|SSS\rangle + |DDD\rangle)$, and the W-state, $|W\rangle = 1/\sqrt{3}\,(|DDS\rangle + |DSD\rangle + |SDD\rangle)$, are representatives (16). The W-state can retain bipartite entanglement when any one of the three qubits is measured in the $\{|S\rangle, |D\rangle\}$ basis, whereas for the maximally entangled GHZ-state a measurement of any one qubit destroys the entanglement. We synthesize the GHZ-state using a sequence of 10 laser pulses and the W-state with a sequence of five laser pulses, respectively (see supporting online material).

Full information on the three-ion entangled states is obtained by state tomography (18, 19) using a CCD camera for the individual detection of ions. The pulse sequences generate three-ion entangled states within less than 1ms. Determining all 64 entries of the

density matrix with an uncertainty of less than 2% requires about 5000 experiments corresponding to 200s of measurement time.

Experimental results for the absolute values of the density matrix elements of GHZ and W-states, $\rho_{|GHZ>}$ and $\rho_{|W>,}$ are displayed in Fig.1a and 1b. The off-diagonal elements are observed with nearly equal height and with the correct phases (see supporting online material: Density matrix elements for GHZ and W-state). Fidelities of 72% for $\rho_{|GHZ>}$ and 83% for $\rho_{|W>}$ are obtained. The fidelity is defined as $|<\Psi_{ideal}|\ \rho_{exp}|\Psi_{ideal}>|^2$ with Ψ_{ideal} denoting the ideal quantum state and ρ_{exp} the experimentally determined density matrix. All sources of imperfections have been investigated independently (13) and the measured fidelities are consistent with the known error budget. Note that for the |W>-state, coherence times greater than 200ms were measured (exceeding the synthesis time by almost three orders of magnitude). This is due to the fact, that W-states are an equal superposition of three states with the same energy and thus the dephasing due to magnetic field fluctuations is much reduced in contrast to a GHZ-state which is maximally sensitive to such perturbations. A similar behaviour has been observed previously with Bell-states (19, 20).

Having tripartite entangled states available as a resource, we make use of individual ion addressing to read out only one of the three ions' quantum state while preserving the coherence of the other two. Qubits are protected from being measured by transferring their quantum information into superpositions of levels which are not affected by the detection, that is a light scattering process. In Ca^+, an additional Zeeman level $D' \equiv D_{5/2}$ (m=-5/2) can be employed for this purpose. Thus, after the state synthesis, we apply two π pulses on the S - D' transition of ion #2 and #3, moving any S population of these ions into their respective D' level. The D and D' levels do not couple to the detection light at 397 nm (see Fig. 2). Therefore, ion #1 can be read out by the electron shelving method as usual (14). After the selective readout a second set of π-pulses on the D' to S transition transfers the quantum information back into the original computational subspace {S, D}.

For a demonstration of this method GHZ- and W-states are generated and the qubits #2 and #3 are mapped onto the {D, D'} subspace. Then, the state of ion #1 is projected onto S or D by scattering photons for a few microseconds on the S-P transition. In a first series of experiments, we did not distinguish whether ion #1 was projected into S or D. After remapping qubits #2 and #3 to the original subspace {S, D}, the tomography procedure is applied to obtain the full density matrix of the resulting three-ion state. As shown in Fig. 1c, the GHZ-state is completely destroyed, i.e. it is projected into a mixture of |SSS> and |DDD>. In contrast, for the W-state, the quantum register remains partially entangled as coherences between ion #2 and #3 persist (see Fig. 1d).

In a second series of experiments with the W-state, we deliberately determine the first ion's quantum state prior to tomography: The ion string is now illuminated for 500μs with light at 397 nm and its fluorescence is collected with a photomultiplier tube, see Fig. 3a. Then, the state of ion #1 is known and subsequently we apply the tomographic procedure to ion #2 and #3 after remapping them to their {S, D} subspace. Depending on the state of ion #1, we observe the two density matrices presented in Fig. 3b and 3c (see supporting online material: Density matrix). Whenever ion #1 was measured in D, ion #2 and #3 were found in a Bell state ($1/\sqrt{2}$ (|SD>+|DS>)), with a fidelity of 82%. If the first qubit was observed in S, the resulting state is |DD> with fidelity of 90%. This is a characteristic signature of W = $1/\sqrt{3}$ (|DDS>+|DSD>+|SDD>): In 1/3 of the cases, the measurement projects qubit #1 into the S state, and consequently the other two qubits are projected into D. With a probability of 2/3 however, the measurement shows qubit #1 in D, and the remaining quantum register is found in a Bell state (16). Experimentally, we observe the first ion in D in 65 (2) % of the cases.

The GHZ-state can be employed to deterministically transform tripartite entanglement into bipartite entanglement using only local measurements and one-qubit operations. For this, we first generate the GHZ-state $1/\sqrt{2}$ (|DSD> + |SDS>). In a second step, we apply a π/2 pulse to ion #1, with phase 3π/2, rotating a state |S> to $1/\sqrt{2}$ (|S> - |D>) and |D> to $1/\sqrt{2}$ (|S> + |D>), respectively. The resulting state of the three ions is $1/\sqrt{2}$ {|D> (|SD> - |DS>) + |S> (|SD> + |DS>)}. A measurement of the first ion, resulting in |D> or |S>,

projects qubits #2 and #3 onto the state (|SD> - |DS>)/$\sqrt{2}$ or the state (|SD> + |DS>)/$\sqrt{2}$, respectively. The corresponding density matrix is plotted in Fig. 4a. With the information of the state of ion #1 available, we can now transform this mixed state into the pure state |S> (|SD> + |DS>)/$\sqrt{2}$ by only local operations. Provided that ion #1 is found in |D>, we perform an appropriate rotation (see online material) on ion #2 to obtain |D>(|SD> + |DS>)/$\sqrt{2}$. In addition, we flip the state of ion #1 to reset it to |S>. Figure 4b shows that the bipartite entangled state |S> (|SD> + |DS>)/$\sqrt{2}$ is produced with a fidelity of 75% (see supporting online material: Density matrix).

Our results prove that selectively reading out a qubit of the quantum register indeed leaves the entanglement of all other qubits in the register untouched. Even after such a measurement has taken place, single qubit rotations can be performed with high fidelity. Such techniques mark a first step towards the one-way-quantum computer, which has been proposed by Briegel et al. (21). First and foremost, we expect that the implementation of unitary transformations conditioned on measurement results has great impact, as it allows for the realization of active quantum-error-correction algorithms, and for deterministic teleportation.

References

1. M. Nielsen and I. Chuang, Quantum computation and quantum information. Cambridge University Press (2000).

2. P. W. Shor, Phys. Rev. **A 52**, R2493 (1995).

3. A. M. Steane, Phys. Rev. Lett. **77**, 793 (1996).

4. C. H. Bennett, D. P. DiVincenzo, J.A. Smolin, and W. K. Wootters, Phys. Rev. **A 54**, 3824 (1996).

5. A. M. Steane, Nature **399**, 124 (1999).

6. C.H. Bennett, G. Brassard, C. Crepeau, R. Jozsa, A. Peres, and W.K. Wootters, Phys. Rev. Lett. **70**, 1895 (1993).

7. A. Rauschenbeutel, G. Nogues, S. Osnaghi , P. Bertet, M. Brune, J. M. Raimond, and S. Haroche , Science **288**, 2024 (2000).

8. C.A. Sackett, D. Kielpinski, B.E. King, C. Langer, V. Meyer, C.J. Myatt, M. Rowe, Q.A. Turchette, W.M. Itano, D.J. Wineland, and C. Monroe, Nature **404**, 256 (2000).

9. J. W. Pan, D. Bouwmeester, M.Daniell, H. Weinfurter and A. Zeilinger, Nature **403**, 515 (2000).

10. J. W. Pan, M. Daniell, S. Gasparoni, G. Weihs, and A. Zeilinger, Phys. Rev. Lett. **86**, 4435 (2001).

11. M. Eibl, N. Kiesel, M. Bourennane, C. Kurtsiefer, and H. Weinfurter, Phys. Rev. Lett. **92**, 077901 (2004).

12. Z. Zhao, Y. Chen, A. Zhang, T. Yang, H. Briegel, and J. W. Pan, http://arXiv.org/abs/ physics/0402096 (2004).

13. F. Schmidt-Kaler, H.Häffner, M. Riebe, S. Gulde, G. P. T. Lancaster, T. Deuschle, C. Becher, C. F. Roos, J. Eschner, and R. Blatt, Nature **422**, 408 (2003).

14. F. Schmidt-Kaler, H. Häffner, S. Gulde, M. Riebe, G. P. T. Lancaster, T. Deuschle , C. Becher, W. Hänsel, J. Eschner, C. F. Roos, and R. Blatt, Appl. Phys. B: Lasers and Optics **77**, 789 (2003).

15. D. M. Greenberger, M. Horne, and A. Zeilinger, in Bell's Theorem, Quantum Theory, and Conceptions of the Universe, edited by M. Kafatos (Kluwer Academic, Dordrecht, 1989).

16. W. Dür, G. Vidal, and J. I. Cirac, Phys. Rev. **A 62**, 062314 (2000).

17. A. Zeilinger, M. A. Horne, and D. M. Greenberger, NASA Conf. Publ. No. 3135 National Aeronautics and Space Administration, Code NTT, Washington, DC, (1997).

18. D. F. V. James, P. G. Kwiat, W. J. Munro, A. G. White, Phys. Rev. A **64**, 052312 (2001).

19. C. F. Roos, G. P. T. Lancaster, M. Riebe, H. Häffner, W. Hänsel, S. Gulde, C. Becher, J. Eschner, F. Schmidt-Kaler, and R. Blatt. Preprint available at http://arXiv.org/abs/ physics/0307210 (2003).

20. D. Kielpinski, V. Meyer, M. A. Rowe, C. A. Sackett, W. M. Itano, C. R. Monroe, and D. J. Wineland, Science **291,** 1013 (2001).

21. R. Raussendorf and H. J. Briegel, Phys. Rev. Lett. **86**, 5188 (2001).

Acknowledgements

We gratefully acknowledge support by the European Commission (QUEST and QGATES networks), by the ARO, by the Austrian Science Fund (FWF), and by the Institut für Quanteninformation GmbH. H.H is funded by the Marie-Curie-program of the European Union. We acknowledge discussions with A. Steinberg, D.F.V James and H. Briegel.

Correspondence and requests for materials should be addressed to:

Ferdinand.Schmidt-Kaler@uibk.ac.at

Figure Legends

Figure 1:

(a) Absolute values of the density matrix elements of the experimentally obtained GHZ quantum state. The off-diagonal elements for SSS and DDD indicate the quantum correlation clearly.

(b) Absolute values of the density matrix of the W-state. Off-diagonal elements are at equal height as the diagonal elements.

(c) GHZ-state after measuring the first qubit only. The GHZ-state coherences have fully disappeared as compared with the results shown in (a). The state is thus fully described by a classical mixture.

(d) W-state after measuring the first qubit. Only the coherences involving the first qubit have disappeared, while two-ion Bell type entanglement persists between the second and the third qubit. The state thus contains quantum correlations even after a local projective measurement.

Figure 2:

Selective read-out of ion #1: Ions #2 and #3 are protected from measurement by transfer into dark states. Only the relevant levels of the three Ca^+ ions are shown.

Figure 3:

a) Histogram of photon counts within 500 μs for ion #1 and threshold setting. b) and c) Density matrix of ion #2 and #3 conditioned upon the previously determined quantum state of ion #1. The absolute values of the reduced density matrix are plotted for ion #1 measured in the S state (b) and ion #1 measured in the D state (c). Off-diagonal elements in (b) show the remaining coherences.

Figure 4:

a) Real part of the density matrix elements of the system after ion #1 of the GHZ-state $1/\sqrt{2}$ (|DSD> + |SDS>) has been measured in a rotated basis. b) Transformation of the GHZ-state $1/\sqrt{2}$ (|DSD> + |SDS>) into the bipartite entangled state $1/\sqrt{2}$ |S>(|DS>+|SD>) by conditional local operations. Note the different vertical scaling of a) and b).

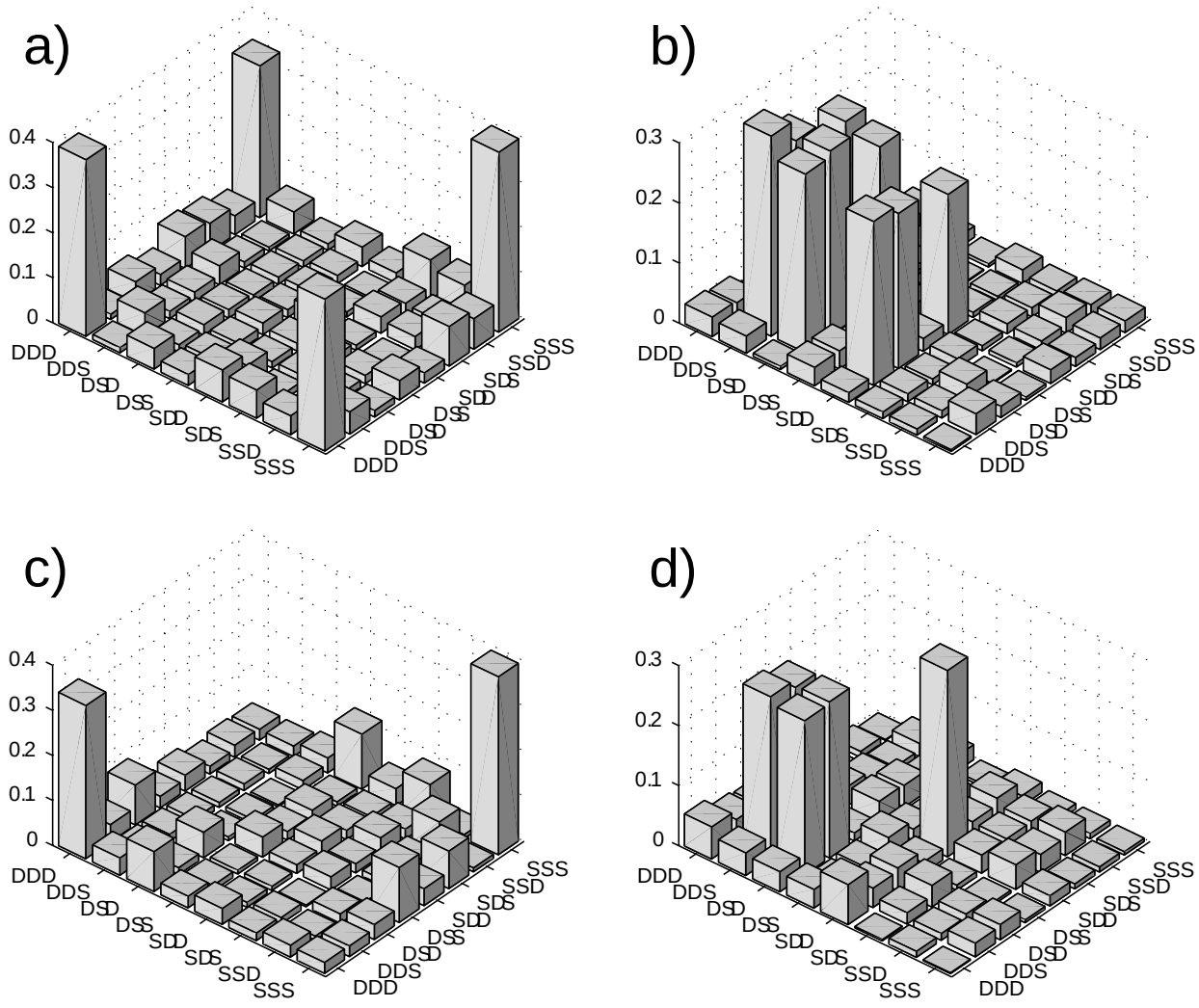
a)
0.4
0.3
0.2
0.1
0
DDD
DDS
DSD
DSS
SDD
SDS
SSD
SSS
b)
0.3
0.2
0.1
0
c)
0.4
0.3
0.2
0.1
0
d)
0.3
0.2
0.1
0

Figure 1

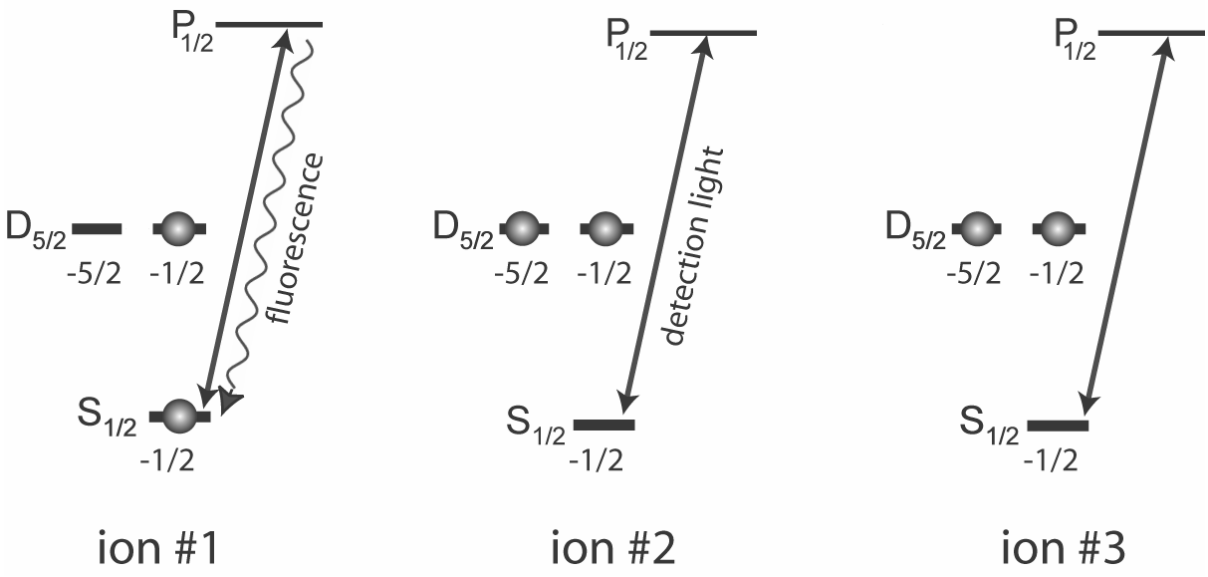
P1/2
D5/2
-5/2
-1/2
fluorescence
S1/2
-1/2
ion #1
P1/2
D5/2
-5/2
-1/2
detection light
S1/2
-1/2
ion #2
P1/2
D5/2
-5/2
-1/2
S1/2
-1/2
ion #3

Figure 2

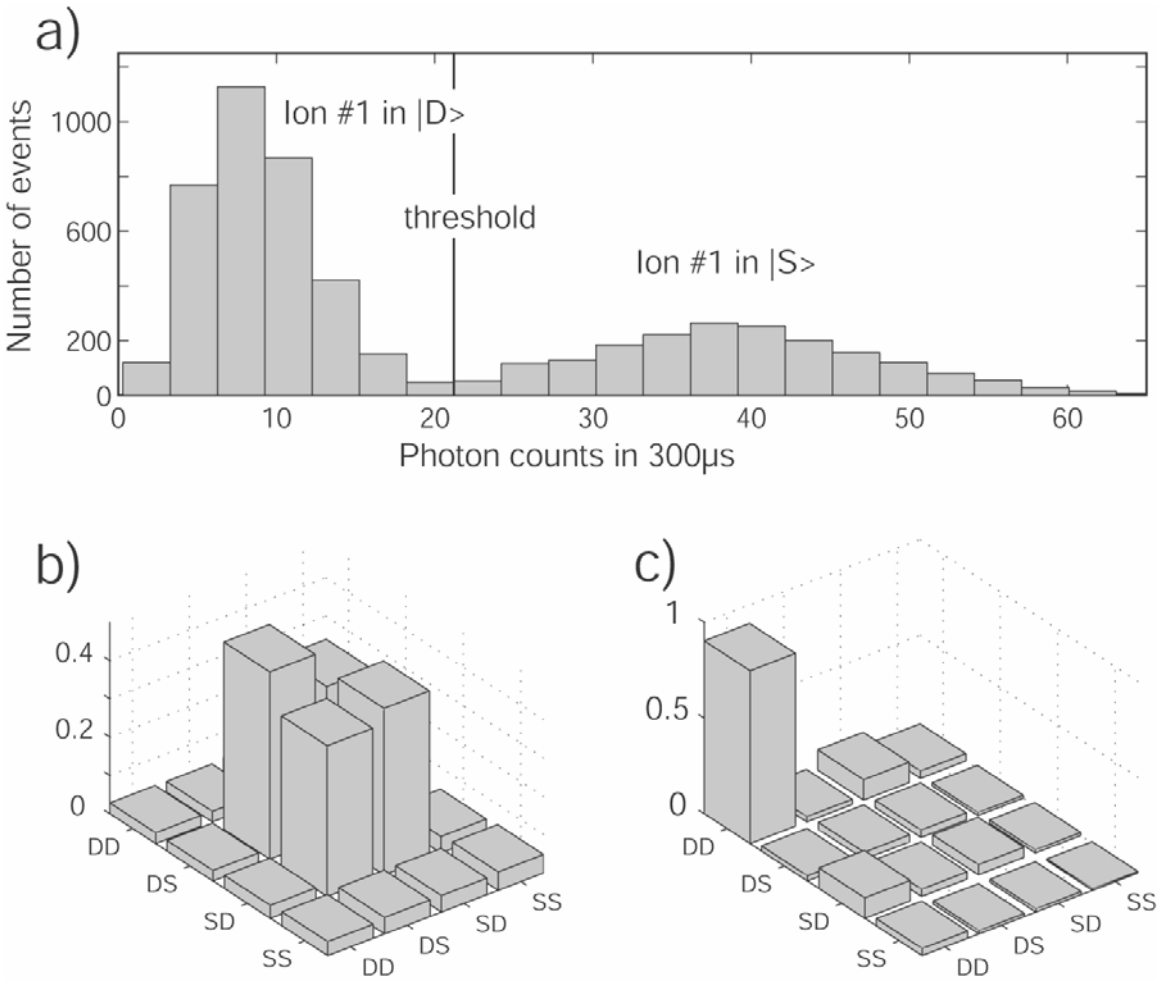
a)
Number of events
1000
600
200
0
0
10
20
30
40
50
60
Photon counts in 300μs
Ion #1 in |D>
threshold
Ion #1 in |S>
b)
0.4
0.2
0
DD
DS
SD
SS
DD
DS
SD
SS
c)
1
0.5
0
DD
DS
SD
SS
DD
DS
SD
SS

Figure 3

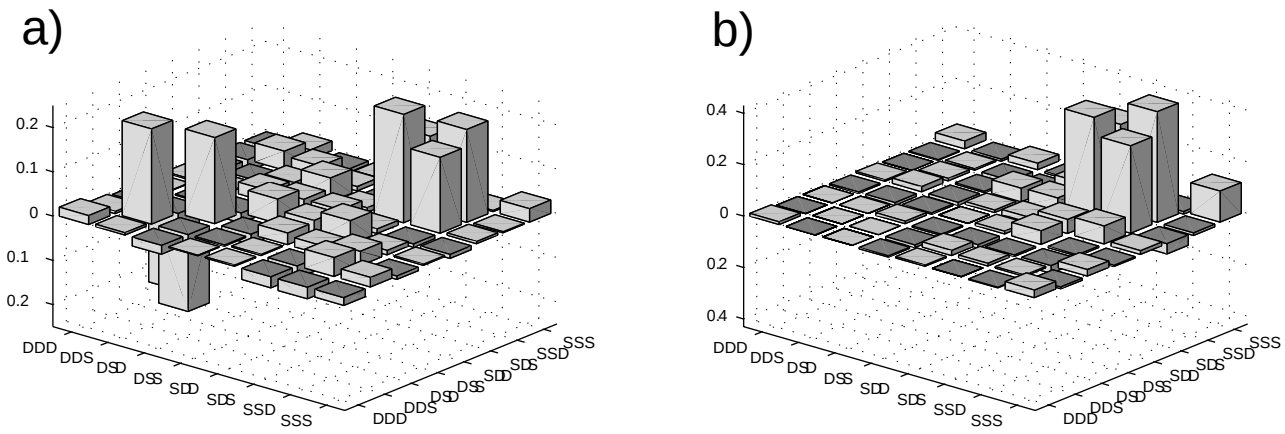
a)
0.2
0.1
0
0.1
0.2
DDD
DDS
DSD
DSS
SDD
SDS
SSD
SSS
b)
0.4
0.2
0
0.2
0.4
DDD
DDS
DSD
DSS
SDD
SDS
SSD
SSS

Figure 4

****

Supporting online material

Pulse notation. Qubit rotations can be written as unitary operations in the following way (1, 2, 3): Carrier rotations are given by $R(\theta,\phi) = \exp\left[i\,\theta/2\left(\mathrm{e}^{i\phi}\,\sigma^{+} + \mathrm{e}^{-i\phi}\,\sigma^{-}\right)\right]$, whereas transitions on the blue sideband are denoted as $R^{+}(\theta,\phi) = \exp\left[i\,\theta/2\left(\mathrm{e}^{i\phi}\,\sigma^{+}b^{\dagger} + \mathrm{e}^{-i\phi}\,\sigma^{-}b\right)\right]$. Here $\sigma^{\pm}$ are the atomic raising and lowering operators which act on the electronic quantum state of the ion by inducing transitions from the |S> to |D> state and vice versa (notation: σ^{+}=|D><S|). The operators b and $b^{\dagger}$ stand for the annihilation and creation of a phonon at the trap frequency, i.e. they work on the motional quantum state. The parameter θ denotes the area of the applied pulse and ϕ is the relative phase between the optical field and the atomic polarization. With the ion prepared in the |S> state, a $R(\pi/2, 0)$ pulse creates the superposition $1/\sqrt{2}$ (|S> + i |D>).

GHZ- and W-state generation. For the creation of a GHZ-state two laser pulses addressed to ion #1 (see Table 1) entangle the ion's electronic state with the vibrational state of the ion crystal: $1/\sqrt{2}$ (|DSS,0> - |SSS,1>), where |XXX,n> denotes the quantum state of the three ions X = {S,D} and the phonon number n = {0,1} of the bus mode. The sequence of 6 pulses addressed to ion #2 performs a zero-controlled CNOT operation with the vibrational quantum number as control qubit and yields $1/\sqrt{2}$ (i|DDS,0> + |SSS,1>). The last two pulses on ion #3 generate the GHZ-state $-1/\sqrt{2}$ (|DDD,0> + |SSS,0>) and return the bus mode back to the vibrational ground state.

Ion #1		Ion #2						Ion #3	
$R_1^{+}(\pi/2,\pi/2)$	$R_1(\pi,\pi/2)$	$R_2(\pi/2,0)$	$R_2^{+}(\pi,\pi/2)$	$R_2^{+}(\pi/\sqrt{2},0)$	$R_2^{+}(\pi,\pi/2)$	$R_2^{+}(\pi/\sqrt{2},0)$	$R_2(\pi/2,\pi)$	$R_3(\pi,0)$	$R_3^{+}(\pi,0)$

Table 1: Pulse sequence to generate a GHZ state. The pulse sequence starts from the left. The duration of the whole sequence is 750 μs.

For a W-state, we apply a "beamsplitter" pulse $R^{+}(2\arccos(1/\sqrt{3}), 0)$ on ion 2 which entangles its quantum state with that of the vibrational bus mode, generating a non-equal superposition $1/\sqrt{3}$ (|SSS,0> + $i\sqrt{2}$ |SDS,1>). The additional laser pulses on ion 3 and 1 yield the W-state $1/\sqrt{3}$ (|DDS,0> + |DSD,0> + |SDD,0>.

Ion #2	Ion #3		Ion #1	
$R_2^+(2\arccos(1/\sqrt{3}), 0)$	$R_3(\pi, \pi)$	$R_3^+(\pi/2, \pi)$	$R_1(\pi, 0)$	$R_1^+(\pi, \pi)$

Table 2: Pulse sequence to generate a |W> state with a duration of 550 μs.

Entanglement transformation. The first pulse R_1 rotates ion #1 such that its subsequent measurement projects the other two ions into one of two Bell states. Provided that ion #1 is found in |D>, we perform a π-rotation of ion #2 about the z-axis which is implemented by two carrier pulses $R_2(\pi,\pi/2)$ and $R_2(\pi,0)$. In addition, we flip the state of ion #1 to reset it to |S>. At the end of this sequence we obtain the pure state |S> (|SD> + |DS>)$/\sqrt{2}$.

Ion #1 measure		Ion #2		Ion #1
$R_1(\pi/2, 3\pi/2)$	$\|S\rangle$	𝟙		𝟙
	$\|D\rangle$	$R_2(\pi, \pi/2)$	$R_2(\pi, 0)$	$R_1(\pi, \pi/2)$

Table 3: Pulse sequence for entanglement transformation.

Matrix elements for GHZ, W and Bell states.

	DDD	DDS	DSD	DSS	SDD	SDS	SSD	SSS
DDD	0.39	-0.01+i*0.01	-0.04+i*0.03	-0.00+i*0.02	-0.07-i*0.02	0.06-i*0.01	0.04+i*0.00	0.33-i*0.09
DDS	-0.01-i*0.01	0.05	0.01-i*0.01	0.02-i*0.00	0.02+i*0.04	0.00+i*0.01	0.01+i*0.00	0.05+i*0.01
DSD	-0.04-i*0.03	0.01+i*0.01	0.02	0.02+i*0.01	-0.00+i*0.01	-0.01+i*0.01	-0.00+i*0.01	-0.01+i*0.01
DSS	-0.00-i*0.02	0.02+i*0.00	0.02-i*0.01	0.03	0.01+i*0.02	0.01+i*0.02	0.01+i*0.01	0.04-i*0.02
SDD	-0.07+i*0.02	0.02-i*0.04	-0.00-i*0.01	0.01-i*0.02	0.05	-0.00+i*0.01	-0.00+i*0.00	-0.02-i*0.00
SDS	0.06+i*0.01	0.00-i*0.01	-0.01-i*0.01	0.01-i*0.02	-0.00-i*0.01	0.04	0.03+i*0.00	0.07-i*0.05
SSD	0.04-i*0.00	0.01-i*0.00	-0.00-i*0.01	0.01-i*0.01	-0.00-i*0.00	0.03-i*0.00	0.03	0.05-i*0.04
SSS	0.33+i*0.09	0.05-i*0.01	-0.01-i*0.01	0.04+i*0.02	-0.02+i*0.00	0.07+i*0.05	0.05+i*0.04	0.40

Density matrix of the GHZ state (c.f. figure 1 a)

	DDD	DDS	DSD	DSS	SDD	SDS	SSD	SSS
DDD	0.03	-0.03-i*0.01	-0.01	0.02-i*0.02	-0.01-i*0.01	0.01-i*0.01	0.01-i*0.00	-0.00-i*0.00
DDS	-0.03+i*0.01	0.33	0.29+i*0.07	-0.02+i*0.02	0.27+i*0.03	-0.01-i*0.01	-0.01+i*0.01	-0.01-i*0.03
DSD	-0.01	0.29-i*0.07	0.31	0.00+i*0.01	0.25-i*0.05	-0.00+i*0.01	-0.03-i*0.01	-0.00-i*0.02
DSS	0.02+i*0.02	-0.02-i*0.02	0.00-i*0.01	0.03	0.00-i*0.02	0.01+i*0.01	0.00+i*0.00	0.00-i*0.00
SDD	-0.01+i*0.01	0.27-i*0.03	0.25+i*0.05	0.00+i*0.02	0.23	-0.01+i*0.00	-0.01-i*0.00	-0.01-i*0.02
SDS	0.01+i*0.01	-0.01+i*0.01	-0.00-i*0.01	0.01-i*0.01	-0.01-i*0.00	0.02	-0.01+i*0.01	0.01-i*0.01
SSD	0.01+i*0.00	-0.01-i*0.01	-0.03+i*0.01	0.00-i*0.00	-0.01+i*0.00	-0.01-i*0.01	0.03	-0.02-i*0.00
SSS	-0.00+i*0.00	-0.01+i*0.03	-0.00+i*0.02	0.00+i*0.00	-0.01+i*0.02	0.01+i*0.01	-0.02+i*0.00	0.02

Density matrix of the W-state (c.f. figure 1 b)

	DD	DS	SD	SS
DD	0.05	0.03+i*0.03	-0.04+i*0.02	0.03-i*0.02
DS	0.03-i*0.03	0.49	0.35-i*0.17	0.02-i*0.02
SD	-0.04-i*0.02	0.35+i*0.17	0.43	-0.03+i*0.02
SS	0.03+i*0.02	0.02+i*0.02	-0.03-i*0.02	0.03

Bell state after detecting ion #1 of the W-state in D (c.f. figure 3 b)

	DDD	DDS	DSD	DSS	SDD	SDS	SSD	SSS
DDD	0.02	-0.01-i*0.01	0.03+i*0.02	-0.00-i*0.01	0.01-i*0.00	0.02-i*0.00	0.03+i*0.02	-0.00-i*0.02
DDS	-0.01+i*0.01	0.21	-0.17+i*0.05	-0.01+i*0.00	0.00-i*0.01	-0.04+i*0.03	0.01-i*0.04	-0.02+i*0.01
DSD	0.03-i*0.02	-0.17-i*0.05	0.19	0.01+i*0.02	0.03+i*0.01	-0.00-i*0.02	0.02-i*0.03	0.01+i*0.01
DSS	-0.00+i*0.01	-0.01-i*0.00	0.01-i*0.02	0.06	-0.02+i*0.03	0.05-i*0.03	0.01+i*0.01	0.02-i*0.00
SDD	0.01+i*0.00	0.00+i*0.01	0.03-i*0.01	-0.02-i*0.03	0.03	0.01-i*0.01	0.02+i*0.01	0.01+i*0.02
SDS	0.02+i*0.00	-0.04-i*0.03	-0.00+i*0.02	0.05+i*0.03	0.01+i*0.01	0.25	0.17-i*0.05	-0.02-i*0.01
SSD	0.03-i*0.02	0.01+i*0.04	0.02+i*0.03	0.01-i*0.01	0.02-i*0.01	0.17+i*0.05	0.21	-0.03-i*0.00
SSS	-0.00+i*0.02	-0.02-i*0.01	0.01-i*0.01	0.02+i*0.00	0.01-i*0.02	-0.02+i*0.01	-0.03+i*0.00	0.03

Mixture of two Bell states after measuring ion #1 of the GHZ-state in a rotated basis (c.f. figure 4 a)

	DDD	DDS	DSD	DSS	SDD	SDS	SSD	SSS
DDD	0.01	0.00+i*0.00	0.00-i*0.00	0.00+i*0.00	-0.00-i*0.00	0.00-i*0.01	-0.00+i*0.01	-0.01+i*0.02
DDS	0.00-i*0.00	0.01	0.01-i*0.00	0.00	0.00+i*0.01	0.04-i*0.01	0.04-i*0.01	0.00+i*0.01
DSD	0.00+i*0.00	0.01+i*0.00	0.01	0.01+i*0.01	-0.00+i*0.01	0.06+i*0.02	0.04+i*0.02	-0.02+i*0.01
DSS	0.00-i*0.00	0.00	0.01-i*0.01	0.02	-0.01+i*0.01	0.03-i*0.03	0.01+i*0.00	0.01+i*0.01
SDD	-0.00+i*0.00	0.00-i*0.01	-0.00-i*0.01	-0.01-i*0.01	0.02	0.01-i*0.05	0.01-i*0.07	-0.01+i*0.00
SDS	0.00+i*0.01	0.04+i*0.01	0.06-i*0.02	0.03+i*0.03	0.01+i*0.05	0.41	0.33-i*0.08	-0.03+i*0.04
SSD	-0.00-i*0.01	0.04+i*0.01	0.04-i*0.02	0.01-i*0.00	0.01+i*0.07	0.33+i*0.08	0.42	0.02+i*0.01
SSS	-0.01-i*0.02	0.00-i*0.01	-0.02-i*0.01	0.01-i*0.01	-0.01-i*0.00	-0.03-i*0.04	0.02-i*0.01	0.11

Bell state after measuring ion #1 of the GHZ-state in a rotated basis and performing local operations conditioned on the measurement result (c.f. figure 4 b)

References (Online Material)

1. F. Schmidt-Kaler, H. Häffner, , M. Riebe, S. Gulde, G.P.T. Lancaster, , T. Deuschle, C. Becher, C. F. Roos, J. Eschner, and R. Blatt, Nature **422**, 408 (2003).

2. S. Gulde, H. Häffner, M. Riebe, G.P.T. Lancaster, C. Becher, J. Eschner, F. Schmidt-Kaler, I. Chuang, and R. Blatt, Phil. Trans. R. Soc. Lond. **A 361**, 1363 (2003).

3. A.M. Childs and I. Chuang, Phys. Rev. **A 63**, 012306 (2001).